JOC Article

Zn(II)-Induced Ground-State π-Deconjugation and Excited-State Electron Transfer in *N*,*N*-Bis(2-pyridyl)amino-Substituted Arenes

Jye-Shane Yang,*,† Yan-Duo Lin,† Yu-Hsi Lin,† and Fen-Ling Liao‡

Department of Chemistry, National Central University, Chung-Li, Taiwan 32054, and Center for Nano Science and Technology, UST, and Instrumentation Center, National Tsing Hua University, Hsinchu, Taiwan 30043

jsyang@cc.ncu.edu.tw

Received January 16, 2004

The synthesis and X-ray crystal structures of two *N*,*N*-bis(2-pyridyl)amino (dpa)-substituted aromatic systems (Ar-dpa) **1** (Ar = 4,4′-disubstituted *trans*-stilbene) and **2** (Ar = 1,4-disubstituted benzene) and their $ZnCl_2$ complexes (**1**/$ZnCl_2$ and **2**/$ZnCl_2$) are reported. The fluoroionophoric behavior of **1**−**2** in response to Zn(II) in acetonitrile also has been investigated. In addition, compound **3DPA** has been prepared and served as a π-deconjugated model for **1DPA**. The observed crystal structures for **1**/$ZnCl_2$ and **2**/$ZnCl_2$ could be divided into two distinct types, the planar and the twisted forms, depending on the aryl−dpa (C_{ph}−NC_3) dihedral angle. The twisted form is more favorable for these complexes unless the arene has a strong "push−pull" character. Nonetheless, the degree of π-conjugation between the *N*-pyridyl and the *N*-aryl group is reduced in both complex forms when compared with the free ligands. Such a Zn(II)-induced π-deconjugation not only directly affects the internal charge transfer (ICT) fluorescence of the dpa-substituted stilbenes but also facilitates the occurrence of photoinduced electron transfer (PET) from the stilbene donor to the dpa/Zn(II) acceptor. The PET process is particularly important in accounting for the observed Zn(II)-induced fluorescence quenching for **1DPA** as well as **3DPA**.

Introduction

The electron donor (D)−acceptor (A) interactions that are associated with light emitting or quenching have demonstrated particular utility in the design of molecule-based fluorescent sensors.[1,2] When the D and A groups are separated by short aliphatic (σ) spacers such as one or two methylene groups, the process of photoinduced electron transfer (PET) in polar solvents generally leads to a loose and nonemissive radical ion pair $D^{+\bullet}A^{-\bullet}$. Thus, a typical PET-based fluorescent chemosensor displays either an "on−off" or an "off−on" fluorescence intensity change in response to analytes.[1] In contrast, for directly linked and π-conjugated D−A systems, the phenomenon of internal charge transfer (ICT) from D to A dominates the electronic absorption and emission properties. As a result of molecular recognitions, not only the intensity but also the position of the fluorescence maximum of an ICT-based sensory molecule could be modulated.[1] Since the electronic (redox) character of an ionophoric D or A can be readily modified upon ion binding, both the PET and the ICT signaling mechanisms are particularly powerful in the construction of fluorescent ion sensors (i.e., fluoroionophores).[2]

The ground-state conformation of D−A systems is known to play a critical role in determining the excited-state behavior and the resulting fluorescence properties.[3,4] For instance, D−A conjugated molecules such as arylamines tend to relax toward a more planar structure in the excited state due to the enhanced electron delocalization interactions, whereas for a largely pretwisted counterpart the twisted angle could be retained or even increased, leading to a twisted ICT (TICT) state with distinct dipole and emission transition moments.[3] Accordingly, structural perturbations, in addition to electrostatic perturbations, as a result of ion recognitions

† National Central University and Center for Nano Science and Technology, UST.

‡ Instrumentation Center, National Tsing Hua University

(1) (a) Czarnik, A. W. *Acc. Chem. Res.* **1994**, *27*, 302−308. (b) de Silva, A. P.; Gunaratne, H. Q. N.; Gunnlaugsson, T.; Huxley, A. J. M.; McCoy, C. P.; Rademacher, J. T.; Rice, T. E. *Chem. Rev.* **1997**, *97*, 1515−1566. (c) Valeur, B.; Leray, I. *Coord. Chem. Rev.* **2000**, *205*, 3−40. (d) de Silva, A. P.; Fox, D. B.; Huxley, A. J. M.; Moody, T. S. *Coord. Chem. Rev.* **2000**, *205*, 41−57. (e) Prodi, L.; Bolletta, F.; Montalti, M.; Zaccheroni, N. *Coord. Chem. Rev.* **2000**, *205*, 59−83. (f) Rurack, K. *Spectrochim. Acta A* **2001**, *57*, 2161−2195. (g) *Handbook of Photochemistry and Photobiology—Supramolecular Chemistry*; Nalwa, H. S., Ed.; American Scientific Publishers: Stevenson Ranch, 2003; Vol. 3.

(2) For recent examples, see: (a) Chen, C.-T.; Huang, W.-P. *J. Am. Chem. Soc.* **2002**, *124*, 6246−6247. (b) Maruyama, S.; Kikuchi, K.; Hirano, T.; Urano, Y.; Nagano, T. *J. Am. Chem. Soc.* **2002**, *124*, 10650−10651. (c) Gawley, R. E.; Pinet, S.; Cardona, C. M.; Datta, P. K.; Ren, T.; Guida, W. C.; Nydick, J.; Leblanc, R. M. *J. Am. Chem. Soc.* **2002**, *124*, 13448−13453. (d) Collado, D.; Perez-Inestrosa, E.; Suau, R.; Desvergne, J.-P.; Bouas-Laurent, H. *Org. Lett.* **2002**, *4*, 855−858. (e) Turfan, B.; Akkaya, E. U. *Org. Lett.* **2002**, *4*, 2857−2859. (f) Zheng, Y.; Gattás-Asfura, K. M.; Konka, V.; Leblanc, R. M. *Chem. Commun.* **2002**, 2350−2351. (g) Kaur, S.; Kumar, S. *Chem. Commun.* **2002**, 2840−2841. (h) Descalzo, A. B.; Martínez-Máñez, R.; Radeglia, R.; Rurack, K.; Soto, J. *J. Am. Chem. Soc.* **2003**, *125*, 3418−3419. (i) Miura, T.; Urano, Y.; Tanaka, K.; Nagano, T.; Ohkubo, K.; Fukuzumi, S. *J. Am. Chem. Soc.* **2003**, *125*, 8666−8671. (j) Nolan, E. M.; Lippard, S. J. *J. Am. Chem. Soc.* **2003**, *125*, 14270−14271. (k) Pearson, A. J.; Xiao, W. *J. Org. Chem.* **2003**, *68*, 5361−5368.

(3) (a) Rettig, W.; Maus, M. *Conformational Analysis of Molecules in Excited States*; Waluk, J., Ed.; Wiley-VCH: New York, 2000; Chapter 1, pp 1−55. (b) Grabowski, Z. R.; Rotkiewicz, K.; Rettig, W. *Chem. Rev.* **2003**, *103*, 3899−4031.

(4) Brouwer, F. *Conformational Analysis of Molecules in Excited States*; Waluk, J., Ed.; Wiley-VCH: New York, 2000; Chapter 4, pp 177−235.

10.1021/jo049902z CCC: $27.50
Published on Web 04/16/2004

should be taken into account for the observed fluoroionophoric properties of PET and ICT probes.[5] Indeed, a twisting of the C−N bond and/or an increase of the degree of pyramidalization of the azacrown nitrogen (D) upon cation binding have been observed for monoazacrown-derived ICT fluoroionophores,[6−8] and in some cases the degree of nitrogen pyramidalization correlates well with the chromoionophoric shift.[6]

We recently reported that *trans*-4-(*N*,*N*-bis(2-pyridyl)-amino)stilbene (**1H**), an "uncrowned" ICT fluoroionophore, undergoes a twisting of the C_{ph}−N bond between the stilbene (A) and the dipyridylamino (dpa, D) moieties upon the binding of transition metal ions by the dpa group (Figure 1a).[9] Such a cation-induced D−A deconjugation process is in accord with the blue-shifted absorption maximum and the weakening of the ICT fluorescence band (415 nm) of **1H** in acetonitrile, particularly in the cases of closed-shell metal ions such as Zn(II) (Figure 1b). While the structures and luminescence properties of many other dpa-substituted arenes (Ar−dpa) and their Zn(II) complexes have been reported,[10−13] the origins of the Zn(II)-complexation effect on the ground-state Ar−dpa conformation and the excited-state D−A interactions are still poorly understood. To gain insights into these two issues, we have synthesized and investigated compounds **1**−**3**. The X-ray crystal structures of compound series **1** and **2** and their complexes **1**/$ZnCl_2$ and **2**/$ZnCl_2$ reported herein indicate that the electronic nature of the aryl group plays an important role in determining the conformation of the complex, where the C_{ph}−N twisted form is more favorable unless the arene possesses a sufficiently strong "push−pull" character. On the basis of the fluorescence behavior of **1DPA** and its D−A non-π-conjugated analogue **3DPA**, we have shown that the dpa/Zn(II) group could act as an electron acceptor. As a result of Zn(II) complexation, the stilbene D−A systems (**1**) become π-deconjugated and the PET process is "turned on", leading to an "on−off" fluorescence response.

Results and Discussion

Synthesis. The synthesis of 4,4′-disubstituted *trans*-stilbene **1DMA** has been recently reported,[5] and that of **1CN** and **1DPA** is outlined in Scheme 1. The conditions

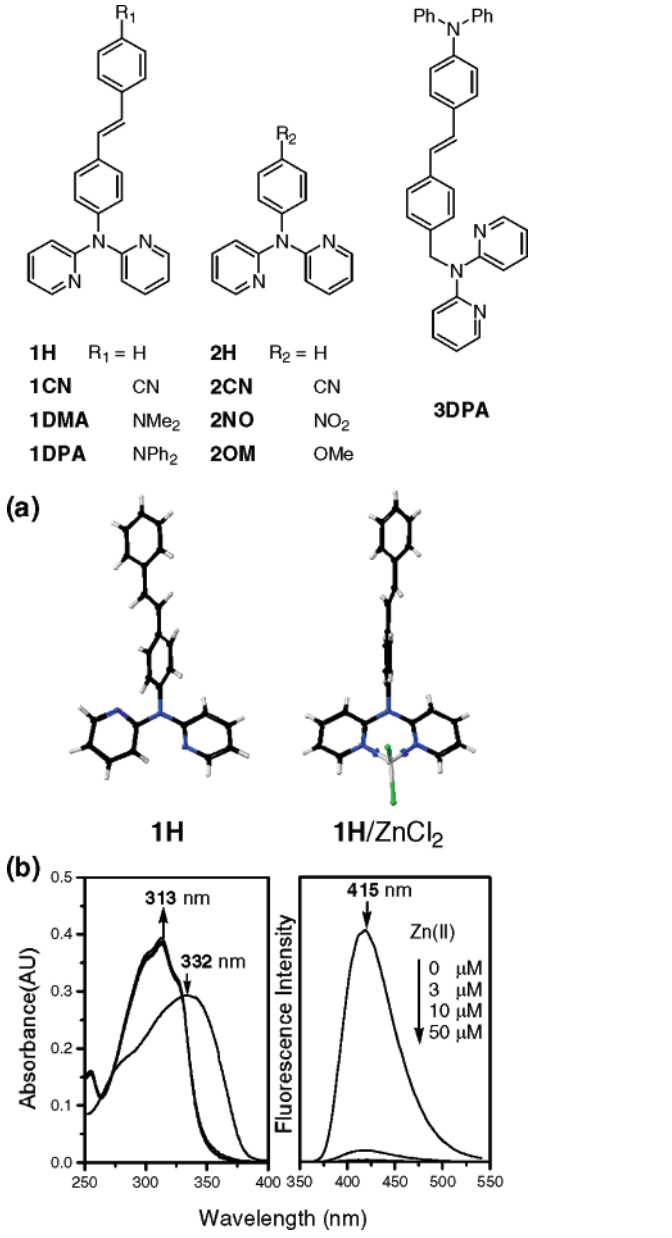

FIGURE 1. (a) Crystal structures of **1H** and **1H**/$ZnCl_2$ and (b) absorption and fluorescence titration spectra of **1H** (10 μM) with Zn(II) (0−5 equiv) in acetonitrile (excitation at 330 nm).

described by Lee and Marvel[14] were adopted for the Wittig reaction to construct the stilbene backbone bearing a nitro group and a cyano (**4CN**) or bromo group (**4Br**) at the para positions. A reduction of the nitro group in **4** by tin(II) chloride[15] produced compound **5**, which was followed by a Pd-catalyzed amination reaction[16] to form compounds **1CN** and **1Br**. Compound **1Br** was then converted to **1DPA** by reacting with diphenylamine under a similar Pd-catalyzed amination condition.

In principle, the series of compound **2** could be prepared by a double *N*-pyridylation of the corresponding

(5) Yang, J.-S.; Hwang, C.-Y.; Hsieh, C.-C.; Chiou, S.-Y. *J. Org. Chem.* **2004**, *69*, 719−726.
(6) Jonker, S. A.; Van Dijk, S. I.; Goubitz, K.; Reiss, C. A.; Schuddeboom, W.; Verhoeven, J. W. *Mol. Cryst. Liq. Cryst.* **1990**, *183*, 273−282.
(7) (a) Rurack, K.; Sczepan, M.; Spieles, M.; Resch-Genger, U.; Rettig, W. *Chem. Phys. Lett.* **2000**, *320*, 87−94. (b) Rurack, K.; Bricks, J. L.; Reck, G.; Radeglia, R.; Resch-Genger, U. *J. Phys. Chem. A* **2000**, *104*, 3087−3109.
(8) Witulski, B.; Weber, M.; Bergsträsser, U.; Desvergne, J.-P.; Bassani, D. M.; Bouas-Laurent, H. *Org. Lett.* **2001**, *3*, 1467−1470.
(9) Yang, J.-S.; Lin, Y.-H.; Yang, C.-S. *Org. Lett.* **2002**, *4*, 777−780.
(10) Yang, W.; Schmider, H.; Wu, Q.; Zhang, Y.-S.; Wang, S. *Inorg. Chem.* **2000**, *39*, 2397−2404.
(11) Wang, S. *Coord. Chem. Rev.* **2001**, *215*, 79−98.
(12) (a) Pang, J.; Marcotte, E. J.-P.; Seward, C.; Brown, R. S.; Wang, S. *Angew. Chem., Int. Ed.* **2001**, *40*, 4042−4045. (b) Seward, C.; Pang, J.; Wang, S. *Eur. J. Inorg. Chem.* **2002**, 1390−1399. (c) Kang, Y.; Seward, C.; Song, D.; Wang, S. *Inorg. Chem.* **2003**, *42*, 2789−2797.
(13) (a) Pang, J.; Freiberg, S.; Yang, X.-P.; D'Iorio, M.; Wang, S. *J. Mater. Chem.* **2002**, *12*, 206−212. (b) Jia, W.-L.; Song, D.; Wang, S. *J. Org. Chem.* **2003**, *68*, 701−705. (c) Liu, Q.-D.; Jia, W.-L.; Wu, G.; Wang, S. *Organometallics* **2003**, *22*, 3781−3791. (d) Du, P.; Li, C.; Li, S.; Zhu, W.; Tian, H. *Synth. Met.* **2003**, *137*, 1131−1132.
(14) Lee, B. H.; Marvel, C. S. *J. Polym. Sci. Chem. Ed.* **1982**, *20*, 393−399.
(15) Bellamy, F. D.; Ou, K. *Tetrahedron Lett.* **1984**, *25*, 839−842.
(16) (a) Wolfe, J. P.; Wagaw, S.; Marcoux, J.-F.; Buchwald, S. L. *Acc. Chem. Res.* **1998**, *31*, 805−818. (b) Hartwig, J. F. *Angew. Chem., Int. Ed.* **1998**, *37*, 2046−2067.

SCHEME 1

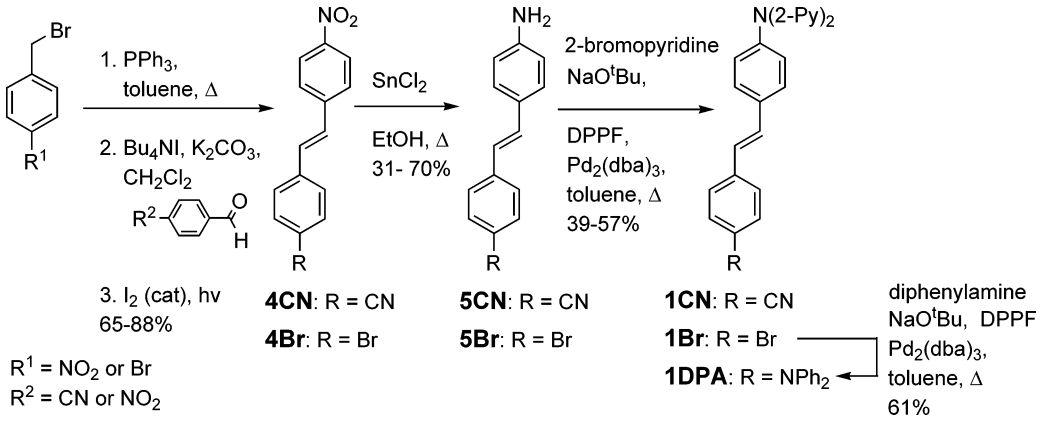

SCHEME 2

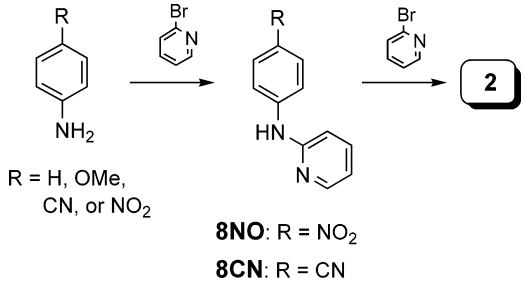

commercially available 4-substitued anilines with 2-bormopyridine under the above-mentioned Pd-catalyzed amination condition (Scheme 2). While this is true in the formation of compounds **2H**, **2CN**, and **2OM**, this method could only afford the monosubstituted adduct **8NO** when 4-nitroaniline was used. It should be also noted that the yield of **2CN** is low (31%) in comparison to those of **2H** (91%) and **2OM** (85%) and, in fact, the monoadduct **8CN** was isolated as the major product (43%) in the *N*-pyridylation of 4-cyanoaniline. Apparently, the efficiency of the second *N*-pyridylation reaction is strongly affected by electron-withdrawing substituents, and it appears that the stronger electron withdrawing the substituent, the less efficient the reaction. These observations are reminiscent of the failure of the Pd-catalyzed amination reaction between 4-bromostilbene and bis(2-pyridyl)-amine for the synthesis of **1H**,[9] because both the 2-pyridyl and 4-nitrophenyl groups are "π-electron-withdrawing" (π-deficient) arenes.[17] It has been recently reported that 2-aminopyridines could tautomerize and form stable hydrogen-bonded dimers of the tautomer (an imine of 2-pyridone) when the group attached to the amino moiety is electron withdrawing.[18] Such a feature of 2-aminopyridines might in part account for the poor Pd-catalyzed amination reactions of **8CN** and **8NO** with 2-bromopyridine. Nonetheless, compound **2NO** could be prepared by using the Ullmann reaction, where Cu(II) and KOH are used as catalysts.[10]

Compound **3DPA** was prepared according to Scheme 3. The starting material **6** was synthesized in a way similar to that for **4** (Scheme 1). The Pd-catalyzed amination reaction between diphenylamine and **6** afforded **7**. A reduction of the ester group in **7** by LAH generated the alcohol **3OH**, which was then converted to **3PI** by the Mitsunobu reaction.[19] The treatment of **3PI** with hydrazine[20] afforded the primary amine **3NH**. The final step in the **3DPA** synthesis was accomplished by the Pd-catalyzed amination reaction between **3NH** and 2-bromopyridine.

The complexation reactions of dpa-substituted arenes **1** and **2** with $ZnCl_2$ were carried out in refluxed acetonitrile/methanol mixed solvents and resulted in **1**/$ZnCl_2$ and **2**/$ZnCl_2$, respectively, in a 1:1 ratio. All the complexes are air stable.

Molecular Structure. Single crystals of ligands **1** and **2** and their complexes of $ZnCl_2$ (**1**/$ZnCl_2$ and **2**/$ZnCl_2$) suitable for X-ray crystallographic studies were grown by slow evaporation of solvent under ambient conditions. The X-ray crystal structures and the corresponding crystallographic details of **1CN**, **1CN**/$ZnCl_2$, **1DMA**, **1DMA**/$ZnCl_2$, **2H**, **2H**/$ZnCl_2$, **2CN**, **2CN**/$ZnCl_2$, **2OM**, **2OM**/$ZnCl_2$, and **2NO**/$ZnCl_2$ are supplied in the Supporting Information.[21] It should be noted that there are two crystallographically independent conformers in the asymmetric unit for free ligands **1H**, **1DMA**, **2H**, and **2OM**

SCHEME 3

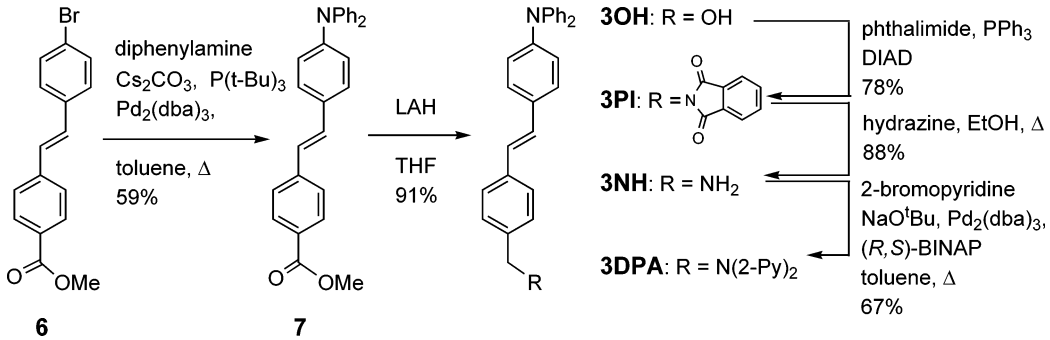

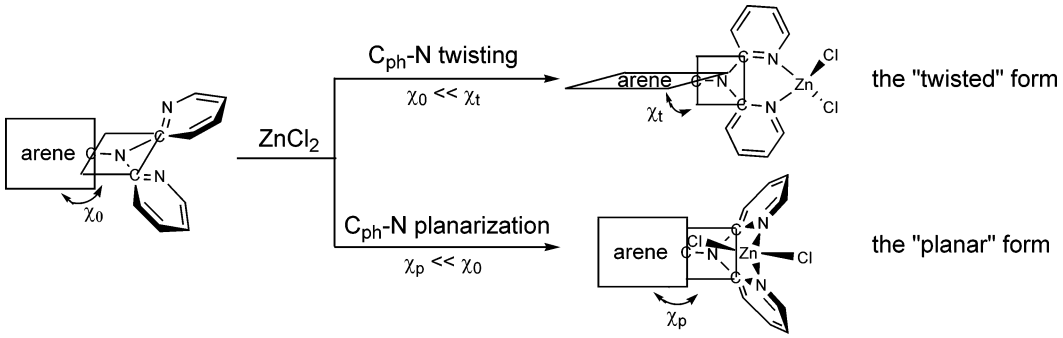

FIGURE 2. Schematic representation of the Zn(II)-induced C_{ph}−N bond twisting and planarization processes in dpa-substituted arenes. Symbols χ_0, χ_p, and χ_t are the dihedral angles between the aryl (phenyl) plane and the NC_3 plane for the free ligand and the planar and the twisted forms of its $ZnCl_2$ complex, respectively.

TABLE 1. Selected Structural Data, Including the Sum of Bond Angles (θ) around the Amino Nitrogen Atom, Dihedral Angles (χ_{ph} and χ_{py}), and C−N Bond Lengths (d_{ph} and d_{py}) in the Triarylamino Moiety for Compounds 1 and 2 and Their $ZnCl_2$ Complexes[a]

compd	θ (deg)	χ_{ph} (deg)	χ_{py} (deg)	d_{ph} (Å)	d_{py} (Å)
1H	359.1	58.5	31.7	1.432	1.409
	359.9	62.8	22.4	1.439	1.412
1CN	359.8	47.4	34.4	1.425	1.413
1DMA	359.9	57.3	31.1	1.433	1.411
	359.8	58.3	25.6	1.439	1.418
2H	359.1	58.7	26.6	1.436	1.408
	359.5	77.8	25.7	1.443	1.405
2CN	357.7	39.0	38.0	1.415	1.425
2OM	359.7	54.3	32.6	1.430	1.409
	359.8	64.2	27.6	1.440	1.407
1H/$ZnCl_2$	359.8	87.6	31.5	1.455	1.414
1CN/$ZnCl_2$	358.6	78.5	28.4	1.468	1.411
1DMA/$ZnCl_2$	359.5	73.9	33.5	1.446	1.415
2H/$ZnCl_2$	359.9	77.4	19.3	1.452	1.409
2CN/$ZnCl_2$	359.6	9.0	70.1	1.411	1.432
	359.4	12.4	69.4	1.408	1.435
2OM/$ZnCl_2$	359.8	87.7	26.9	1.452	1.413
2NO/$ZnCl_2$	359.9	5.1	68.6	1.437	1.428
	360.0	11.9	67.1	1.422	1.426

[a] Two sets of data are provided for those having two independent conformers in the crystals.

and for complexes **2CN**/$ZnCl_2$ and **2NO**/$ZnCl_2$, but only one of the two conformers is shown for these cases. The difference between the two conformers is small except for the case of **2H** (vide infra).

Selected structural data for **1** and **2** and their complexes are given in Table 1. As evaluated by the sum of bond angles (θ) about the amino nitrogen, the amino nitrogen atom is essentially coplanar (NC_3 plane) with the three carbon atoms to which it attaches in all cases ($\theta \sim 360°$). The three *N*-aryl rings (one *N*-phenyl and two *N*-pyridyl rings) in free ligands **1** and **2** have a propeller arrangement, which could be attributed to steric interactions between them. A change in the tilted orientation of such a propeller arrangement, either clockwise or counterclockwise, accounts for the primary difference between the two crystallographically independent conformers for **1H**, **1DMA**, **2H**, and **2OM**. It is noted that the dihedral angle (χ_{ph}) between the central NC_3 plane and the *N*-phenyl plane is smaller for **2CN**, but the average of its two dihedral angles (χ_{py}) between the NC_3 plane and the *N*-pyridyl rings is relatively larger. In addition, the χ_{ph} value in one of the two conformers of **2H** is 77.8°, significantly larger than that in the other conformer (58.7°) and those in the other free ligands (39.0−64.2°). The relative C_{ph}−N bond length (d_{ph}) and the average of the two C_{py}−N bond lengths (d_{py}) appear to parallel the relative χ_{ph} and χ_{py} values (Table 1). As judged by the dihedral angle (α) between the two phenyl rings, the stilbene moiety is more planar in **1CN** (6°) than that in **1H** (21−35°) and **1DMA** (13−30°). Regarding the structures of the complexes, the geometry of the Zn(II) ion in all cases is a distorted tetrahedron with N−Zn−N bond angles (87.9−90.9°) and Zn−N bond lengths (2.016−2.066 Å) similar to those in the previously reported Ar−dpa/$ZnCl_2$ complexes.[10−12] When compared with the corresponding free ligands, the stilbene moiety in **1H**/$ZnCl_2$ (α = 34°) and **1CN**/$ZnCl_2$ (α = 3°) is not much perturbed, but it becomes more planar in **1DMA**/$ZnCl_2$ (α = 3°). More intriguing changes are in the triarylamino moiety, where the χ_{ph} value either increases or decreases to a large extent, leading to two distinct geometries. As depicted in Figure 2, an increase in χ_{ph} results in a nearly orthogonal conformation between the *N*-phenyl and the dpa groups (the "twisted" form), as observed for all three stilbene complexes and for **2H**/$ZnCl_2$ and **2OM**/$ZnCl_2$ (χ_{ph} = 74−88°). In contrast, the χ_{ph} value is relatively small in **2CN**/$ZnCl_2$ and **2NO**/$ZnCl_2$ (5−13°), and the conformation is thus referred to as the "planar" form. Since both the cyano and the nitro substituents are strong electron-withdrawing groups, it appears that the planar form is favorable only when the aryl group has a strong "push−pull" character. It should be noted that the χ_{py} value is significantly increased with the decrease of χ_{ph}. As a result, no matter which form is adopted by the complex, the degree of π-conjugation between the *N*-aryl and the *N*-pyridyl groups is largely reduced on going from the free ligands to the Zn(II) complexes (Figure 3).

An elegant balance between the steric and electronic conjugation (delocalization) interactions in the triarylamino moiety might account for the substituent effect on the conformation of these complexes.[22] For the free ligands, a coplanar geometry of the triarylamino moiety

(17) (a) Abbotto, A.; Bradamante, S.; Pagani, G. A. *J. Org. Chem.* **1993**, *58*, 444−448. (b) Abbotto, A.; Bradamante, S.; Facchetti, A.; Pagani, A. *J. Org. Chem.* **2002**, *67*, 5753−5772.

(18) Alkorta, I.; Elguero, J. *J. Org. Chem.* **2002**, *67*, 1515−1519.

(19) Mitsunobu, O. *Synthesis* **1981**, 1−28.

(20) Sheehan, J. C.; Bolhofer, W. A. *J. Am. Chem. Soc.* **1950**, *72*, 2786−2788.

(21) A good quality of single crystals of **2NO** was not available, and the quality of crystals of **2NO**/$ZnCl_2$ was less satisfactory due to the presence of twinning. Nonetheless, a reasonable structure could be derived from the X-ray diffraction data.

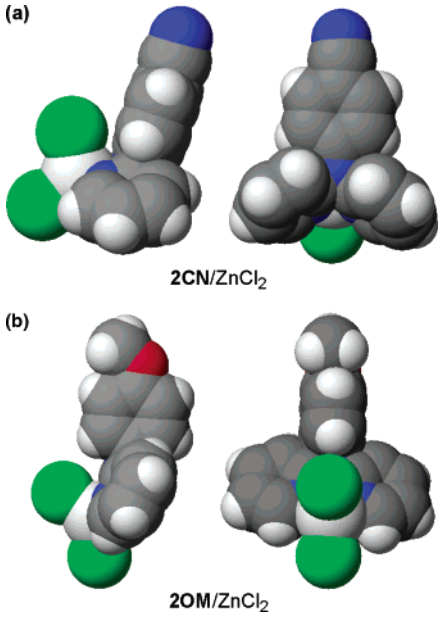

FIGURE 3. Two views of the crystal structures (space-filling model) of (a) **2CN**/$ZnCl_2$ and (b) **2OM**/$ZnCl_2$ to show the orientation of the *N*-aryl and *N*-pyridyl groups in the planar and the twisted forms of complexes, respectively.

would have the maximum conjugation interaction, but it would also encounter the most sever steric hindrance. A compromise of these two effects thus leads to a propeller arrangement of the three *N*-aryl groups. On the basis of the relative values of the $C_{ph}-NC_3$ dihedral angles (χ) and the C−N bond lengths (d) (Table 1), the conjugation interaction of the amino nitrogen lone-pair electrons with the *N*-aryl groups appears to be stronger (i.e., smaller χ and d values) in the pyridylamino than in the arylamino group in all free ligands except for those having electron-withdrawing substituents in the aryl group. The arylamino vs pyridylamino conjugation interaction seems comparable in **1CN** and **2CN**. Upon complexation with Zn(II), the propeller arrangement of the triarylamino group is perturbed (Figure 2). In the planar form of complexes, the conjugation interaction is enhanced in the arylamino group but diminished in the pyridylamino group. However, the reverse is true in the twisted form. Given the fact that the binding of Zn(II) by the dpa moiety will further enhance the charge-delocalization interactions in the pyridylamino group, the twisted form should be more favorable than the planar form in terms of the conjugation effect. While this could account for the observed twisted form for **1H**/$ZnCl_2$, **1DMA**/$ZnCl_2$, **2H**/$ZnCl_2$, and **2OM**/$ZnCl_2$, the choice of the planar form by **2CN**/$ZnCl_2$ and **2NO**/$ZnCl_2$ indicates that the electron-withdrawing CN and NO_2 substituents provide sufficient driving force for conjugation that the aniline lone pair remains conjugated. Despite the presence of a CN substituent, **1CN**/$ZnCl_2$ adopts the twisted form. This could be attributed to a relatively weak long-rang conjugation interaction in the arylamino group due to the larger separation of the D and A groups.

(22) Other noncovalent interactions such as Cl···H−C (in the twisted form) or Cl···π (in the planar form) should be weak due to the lack of close contact.

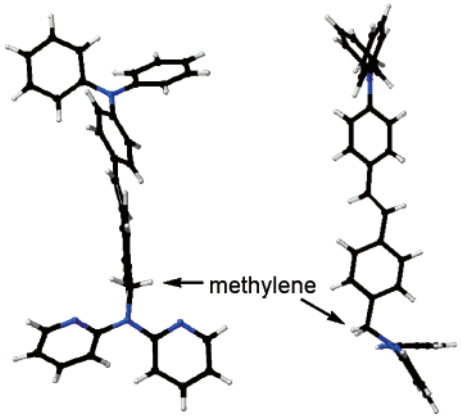

FIGURE 4. Two views of the X-ray crystal structure of **3-DPA**.

The crystal structure of the arene−dpa non-π-conjugated derivative **3DPA** was also determined (Figure 4). The presence of a methylene group between the stilbene and the dpa group does not affect the geometry of the dpa group as compared with that in **1** and **2**. The dpa nitrogen atom is sp^2-hybridized with a θ value of 359.9°, and the values of χ_{py} and d_{py} are 31.5° and 1.402 Å, respectively. It is interesting to note that the dpa group is nearly orthogonal (85°) to the adjacent phenyl ring of stilbene. The nitrogen atom in the diphenylamino group has as expected[23] a trigonal planar geometry with θ = 359.4°. An attempt to grow single crystals for **3DPA**/$ZnCl_2$ was unfortunately unsuccessful.

Electronic Spectra and Zn(II)-Induced Spectral Responses. The absorption and fluorescence spectra of the dpa-substituted stilbenes **1** in the absence and the presence of Zn(II) in acetonitrile have been investigated. As shown in Table 2, the large Stokes shifts in all four free ligands, including the donor−donor-type stilbenes **1DMA** and **1DPA**, indicate the presence of strong ICT upon electronic excitation.[5] The strong fluorescence of **1H** is a result of the "amino conjugation effect" observed for *N*-aryl-substituted *trans*-4-aminostilbenes.[23] Compound **1DPA** is also strongly fluorescent with a quantum efficiency similar to those for **1H** and *trans*-tetramethyldiaminostilbene (Φ_F = 0.57 in MeCN).[24] For compounds **1CN** and **1DMA**, their fluorescence quantum yields are relatively lower, which could be attributed to the presence of a strong electron-withdrawing cyano (**1CN**) or an electron-donating dimethylamino (**1DMA**) group. A study of substituent effect on the fluorescence quantum yield of *trans*-4,4′-disubstituted stilbenes has been reported.[25] Despite the different nature of these substituted stilbene fluorophores, all four compounds display the same fluoroionophoric behavior in response to the presence of Zn(II) in acetonitrile: namely, most of the ICT fluorescence is quenched upon the addition of 1 equiv of Zn(II), as represented by the case of **1H** (Figure 1b) and **1DPA** (Figure 5).[26] It should be noted that the Zn(II)-induced

(23) (a) Yang, J.-S.; Chiou, S.-Y.; Liau, K.-L. *J. Am. Chem. Soc.* **2002**, *124*, 2518−2527. (b) Yang, J.-S.; Wang, C.-M.; Hwang, C.-Y.; Liau, K.-L.; Chiou, S.-Y. *Photochem. Photobiol. Sci.* **2003**, *2*, 1225−1231.

(24) Létard, J.-F.; Lapouyade, R.; Rettig, W. *J. Am. Chem. Soc.* **1993**, *115*, 2441−2447.

(25) Papper, V.; Pines, D.; Likhtenshtein, G.; Pines, E. *J. Photochem. Photobiol. A: Chem.* **1997**, *111*, 87−96.

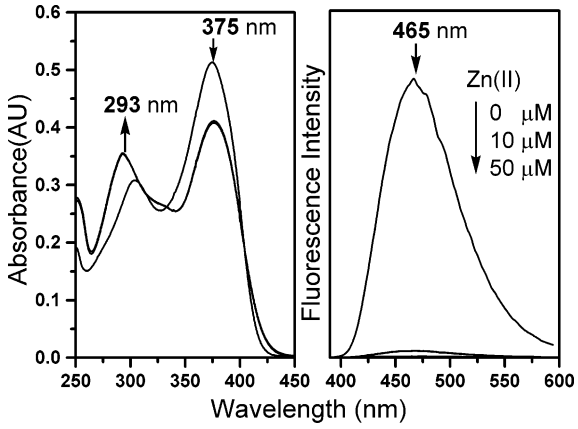

FIGURE 5. Absorption and fluorescence titration spectra of **1DPA** (10 μM) with Zn(II) (0−5 equiv) in acetonitrile (excitation at 375 nm).

TABLE 2. Maxima of UV−Vis Absorption (λ_{abs}) and Corrected Fluorescence (λ_{fl}), Fluorescence-Band Half-Width ($\Delta\nu_{1/2}$), Stokes Shift ($\Delta\nu_{st}$), and Fluorescence Quantum Yields (Φ_f) of Compounds 1−3, 1/Zn(II)−3/Zn(II),[a] and DPhAS in Acetonitrile at Room Temperature (ca. 298 K)

compd	λ_{abs} (nm)	λ_{fl} (nm)	$\Delta\nu_{1/2}$ (cm^{-1})	$\Delta\nu_{st}$ (cm^{-1})[b]	Φ_f
1H	332	415	3483	6024	0.60
1H/Zn(II)	313	415	3614		
1CN	360	492	3542	7453	0.19
1CN/Zn(II)	321	487	3644		
1DMA	368, 338	454	3436	5147	0.12
1DMA/Zn(II)	368	461	3737		
1DPA	375, 304	465	3602	5161	0.64
1DPA/Zn(II)	376, 293	472	4428		
2H	295, 273	385	3888	7924	0.07
2H/Zn(II)	321, 291	387	4081		
2OM	298, 272	440	4898	10830	0.07
2OM/Zn(II)	322, 287	457	5780		
2CN	321	398	4123	6027	0.32
2CN/Zn(II)	319, 282	400	4682		
2NO[c]	378, 296				
2NO/Zn(II)[c]	322, 288				
3DPA	365, 299	464	3609	5846	0.68
3DPA/Zn(II)	368, 294	466	3822		
DphAS	362	463	3773	6026	0.66
dpaH/Zn(II)[d]	315	360		3968	0.12

[a] Data determined with **1**−**3**:Zn(II) = 1:5. [b] $\Delta\nu_{st} = \nu_{abs} - \nu_{fl}$ of spectral maxima. [c] Fluorescence too weak to be determined. [d] Data from ref 29.

spectral changes for **1CN** and **1DMA** resemble those for **1H** and **1DPA**, respectively. When compared with the absorption spectra of **1H**, Zn(II) complexation has a much smaller effect on the long-wavelength absorption maximum of **1DPA** but spectral broadening on the red edge is more prominent. A study of ion selectivity by the dpa group based on the relative extent of fluorescence quenching for **1H** has been reported in a preliminary account of this work.[9] The choice of Zn(II) for the current mechanistic study on the fluoroionophoric properties of **1** is mainly due to the negligible external fluorescence-quenching effect of Zn(II).[27] Thus, the observed fluorescence quenching should result from the perturbation of the electronic and structural properties of **1** by Zn(II).

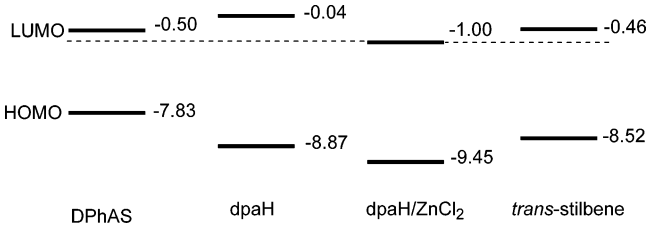

FIGURE 6. Tha AM1-calculated energies (eV) for the HOMO and LUMO of DPhAS, dpaH, dpaH/$ZnCl_2$, and *trans*-stilbene in the gas phase.

The Zn(II)-induced fluorescence quenching for **1H** has been correlated to the deconjugation of the stilbene group from the dpa group (Figure 1), which interrupts the ICT process and the *N*-pyridyl conjugation effect.[9,23] According to the above structural analysis for **1**/$ZnCl_2$ and **2**/$ZnCl_2$, a π-deconjugation of the *N*-pyridyl group from the stilbene fluorophore appears to be inevitable when these dpa-substituted stilbenes bind Zn(II) (Figure 3). However, such a π-deconjugation process alone seems not sufficient to account for the fluorescence-quenching responses of these stilbene derivatives to Zn(II), particularly in the case of **1DPA** (Figure 5). If the conformational effect alone was in operation, the fluorescence spectrum of **1DPA** would not be much affected by the presence of Zn(II), because the fragment of *N*,*N*-diphenylaminostilbene (DPhAS) is known to be strongly fluorescent with a quantum yield and fluorescence maximum similar to those of the **1DPA** molecule (Table 2).[23] Apparently, new pathways of nonradiative decay have been triggered when these dpa-substituted stilbenes interact with Zn(II).

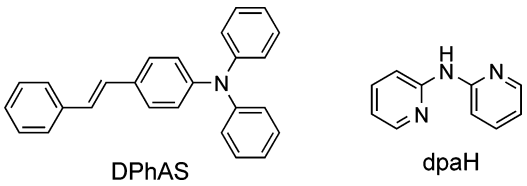

We thus ascribe the Zn(II)-induced fluorescence quenching for **1DPA** to a result of PET from the DPhAS moiety to the dpa/Zn(II) moiety. This is supported by the AM1-calculated energies of the frontier orbitals for DPhAS, dpaH, and dpaH/$ZnCl_2$ (Figure 6).[28] The highest occupied molecular orbital (HOMO) and the lowest unoccupied molecular orbital (LUMO) of dpaH were calculated to lie below and above the corresponding HOMO and LUMO of DPhAS, respectively. Accordingly, the PET between the locally excited DPhAS and the ground-state dpaH would be an unfavorable endothermic process. However, the energies of both the HOMO and LUMO of dpaH/$ZnCl_2$ are lower than the HOMO and LUMO of dpaH, respectively, in analogy to the results for the other dpa derivatives based on ab initio calculations.[10] This thus allows an exothermic PET process from the LUMO of

(26) The previously observed[9] weak fluorescence grown in the blue region at ca. 344 nm accompany the quenching of ICT fluorescence by Zn(II) in the case of **1H** was no longer observed when a fresh acetonitrile solution of $Zn(ClO_4)_2 \cdot 6H_2O$ was used.

(27) Varnes, A. W.; Dodson, R. B.; Wehry, E. L. *J. Am. Chem. Soc.* **1972**, *94*, 946−950.

(28) (a) MOPAC-AM1 calculations were performed on a personal computer, using the algorithms supplied by the package of Quantum CAChe Release 3.2, a product of Fujitsu Limited. (b) Dewar, M. J. S.; Zoebisch, E. G.; Healy, E. F.; Stewart, J. J. P. *J. Am. Chem. Soc.* **1985**, *107*, 3902−3909.

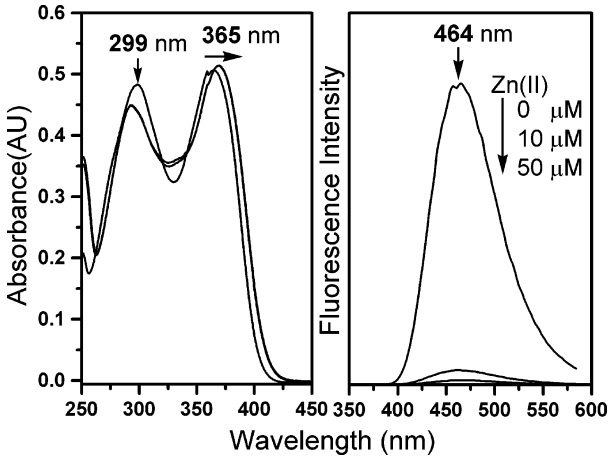

FIGURE 7. Absorption and fluorescence titration spectra of **3DPA** (10 μM) with Zn(II) (0−5 equiv) in acetonitrile (excitation at 365 nm).

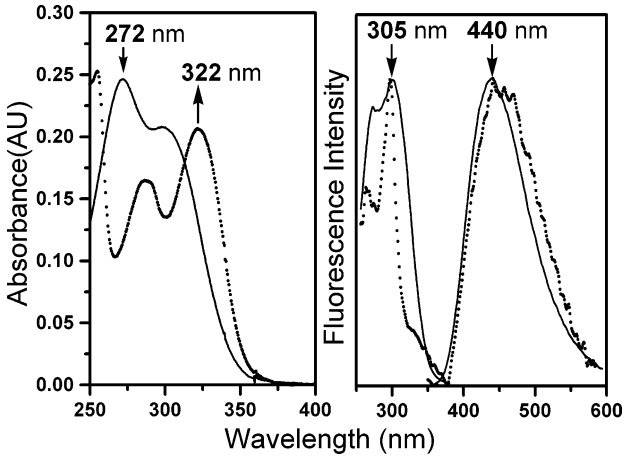

FIGURE 8. Absorption and normalized excitation (emission at 460 nm) and emission (excitation at 300 nm) spectra of **2OM** (10 μM) in the absence (full line) and the presence (dot line) of 5 equiv of Zn(II) (50 μM) in acetonitrile.

DPhAS to the LUMO of dpaH/Zn(II) when the DPhAS is electronically excited.

To gain experimental evidence for the occurrence of PET in **1DPA**/Zn(II), the fluoroionophoric behavior of the corresponding non-π-conjugated D−A analogue **3DPA** has been investigated. The structure of **3DPA** nicely mimics the π-deconjugated conformation of **1DPA**, due to the presence of a methylene group between the DPhAS and the dpa groups (Figure 4). In the absence of Zn(II), **3DPA** is strongly fluorescent with a feature similar to DPhAS (Table 2), indicating that the DPhAS fluorophore has negligible interactions with the dpa group. Like the case of **1DPA**, the ICT fluorescence of **3DPA** is largely quenched upon the addition of Zn(II) (Figure 7). These observations clearly demonstrate that the dpa/Zn(II) group interacts with the excited DPhAS fluorophore and then quenches its fluorescence. Fluorescence quenching resulting form an energy transfer from the excited DPhAS to the dpa/Zn(II) is unlikely in **1DPA**/$ZnCl_2$ and **3DPA**/$ZnCl_2$, because of the absence of spectral overlap of the DPhAS emission and the dpaH/Zn(II) absorption (Table 2).[29] On the other hand, the occurrence of PET from the DPhAS donor to the dpa/Zn(II) acceptor is theoretically allowed (Figure 6), and an induction of PET as a result of Zn(II) complexation has been previously observed for 4-(dialkylamino)pyrimidines (4-DMAP).[30] The presence of PET in directly linked but π-deconjugated (orthogonal) D−A systems has long been proposed for some twisted systems related to *N,N*-dimethylaminobenzonitrile (e.g., TMABN).[3] A recent example has been provided by fluorescein derivatives.[31] A combination of ICT and PET signaling mechanisms for the formation of fluoroionophores that possess both of the features of sensitivity (PET) and spectral shift (ICT) has been reported.[32] Thus, the Zn(II)-induced intramolecular PET is more likely the main origin responsible for the "on−off" fluorescence response of the ICT-based probe **1DPA**.

It is interesting to point out that the non-π-conjugated dpa analogue, bis(2-pyridylmethyl)amine (di-2-picolylamine, dpma), is also a good ionophore for Zn(II) and has been used to form PET-based fluorescent probes.[33] The participation of the amino nitrogen of dpma in the binding of Zn(II) accounts for their "off−on" fluorescence response.

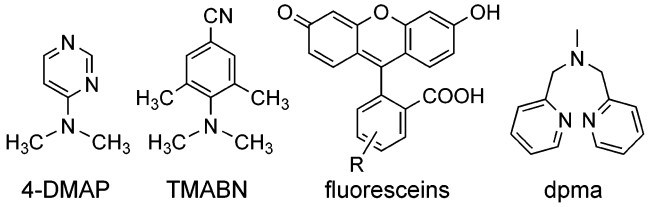

For comparison, the electronic spectra of compound series **2** (10 μM) in the absence and the presence of Zn(II) (50 μM) in acetonitrile have also been investigated. The spectra of **2OM** are shown in Figure 8 and the spectroscopic data of all four compounds are collected in Table 2. The fluorescence of **2NO** is too weak to be determined, presumably due to an efficient intersystem crossing promoted by the nitro group.[34] The shorter conjugation length of **2H** vs **1H** and **2CN** vs **1CN** is consistent with the blue-shifted absorption and fluorescence maxima. The Stokes shift of compounds **2** in acetonitrile is also significant; however, the substituent effect on the Stokes shift shows an opposite trend in **2** vs **1**, i.e., **2OM** > **2H** > **2CN** but **1DMA** < **1H** < **1CN**. As a result, despite the great similarity in absorption spectrum between **2OM**

(29) (a) Ho, K.-Y.; Yu, W.-Y.; Cheung, K.-K.; Che, C.-M. *Chem. Commun.* **1998**, 2101−2102. (b) Ho, K.-Y.; Yu, W.-Y.; Cheung, K.-K.; Che, C.-M. *J. Chem. Soc., Dalton Trans.* **1999**, 1581−1586.

(30) Herbich, J.; Grabowski, Z. R.; Wójtowicz, H.; Golankiewicz, K. *J. Phys. Chem.* **1989**, *93*, 3439−3444.

(31) Miura, T.; Urano, Y.; Tanaka, K.; Nagano, T.; Ohkubo, K.; Fukuzumi, S. *J. Am. Chem. Soc.* **2003**, *125*, 8666−8671.

(32) (a) Rurack, K.; Resch-Genger, U.; Bricks, J. L.; Spieles, M. *Chem. Commun.* **2000**, 2103-2104. (b) Rurack, K.; Bricks, J. L.; Schulz, B.; Maus, M.; Reck, G.; Resch-Genger, U. *J. Phys. Chem. A* **2000**, *104*, 6171−6188. (c) Rurack, K.; Danel, A.; Rotkiewicz, K.; Grabka, D.; Spieles, M.; Rettig, W. *Org. Lett.* **2002**, *4*, 4647−4650.

(33) (a) Walkup, G. K.; Burdette, S. C.; Lippard, S. J.; Tsien, R. Y. *J. Am. Chem. Soc.* **2000**, *122*, 5644−5645. (b) Hirano, T.; Kikuchi, K.; Urano, Y.; Higuchi, T.; Nagano, T. *J. Am. Chem. Soc.* **2000**, *122*, 12399−12400. (c) Burdette, S. C.; Walkup, G. K.; Spingler, B.; Tsien, R. Y.; Lippard, S. J. *J. Am. Chem. Soc.* **2001**, *123*, 7831−7841. (d) Ojida, A.; Mito-oka, Y.; Inoue, M.; Hamachi, I. *J. Am. Chem. Soc.* **2002**, *124*, 6256−6258.

(34) Munkholm, C.; Parkinson, D.-R.; Walt, D. R. *J. Am. Chem. Soc.* **1990**, *112*, 2608−2612.

and **2H**, the fluorescence spectrum of **2OM** is relatively broader with a maximum (440 nm) at longer wavelength than those of **1H** (415 nm) and **2H** (385 nm). These features indicate that the excited states of **2** have a large ICT character and the direction of transition moment in **2** is different from that in **1**. In the presence of Zn(II), the absorption spectra of **2** shift to either blue (**2CN** and **2NO**) or red (**2H** and **2OM**), resulting in similar absorption maxima for **2**/Zn(II). Like the cases of **1**, the ICT fluorescence of **2H** and **2CN** is broadened and mostly quenched (85−99%). The ICT fluorescence of **2OM** is also largely reduced (95%) by Zn(II), but the residual fluorescence maximum is significantly red-shifted, from 440 to 457 nm. In views of the D−A pretwisted structures of **2**/Zn(II), the formation of an weakly fluorescent TICT state might account for these results.[3]

The frontier orbitals of *trans*-stilbene have also been investigated and compared with those of dpaH/$ZnCl_2$ (Figure 6). Like the case of DPhAS vs dpaH/$ZnCl_2$, both the AM1-calculated HOMO and LUMO of *trans*-stilbene lie above those of dpa/$ZnCl_2$, respectively, indicating that the process of PET could also take place in **1H**/$ZnCl_2$. Therefore, a full account of the mechanism of Zn(II)-induced fluorescence quenching for stilbenes **1** should include (1) the ground-state π-deconjugation between the dpa and the stilbene groups that interrupts the ICT process in the aminostilbene fluorophore and (2) the occurrence of PET from the stilbene donor to the dpa/Zn(II) acceptor that presumably results in a nonemissive radical ion pair.

Concluding Remarks

This work has provided insights into the Zn(II)-complexation effect on the structures and fluorescence properties of the dpa-derived stilbene probes **1** based on systematic studies of **1**−**3** in the absence and the presence of Zn(II). The X-ray crystal structures of dpa-substituted arenes **1** and **2** and their $ZnCl_2$ complexes have shown that Zn(II)-complexation results in either the "planar" or the "twisted" structure with a preference for the latter, presumably due to a better conjugation interaction in the dpa/Zn(II) vs the arylamino group. When the aryl group possesses a sufficiently strong push−pull character, the planar form would become more favorable. However, no matter which form is adopted, the two *N*-pyridyl groups always become much less π-conjugated with the aryl group on going from the free ligands to the complexes. It should be noted that, unlike the cases of free ligands, structural relaxation of the complexes toward a more π-conjugated conformation in the excited state will be small or negligible due to the rigid and pretwisted structure of the dpa/Zn(II) group. While such a structural perturbation by Zn(II) can directly interrupt the amino conjugation effect[23] and thus reduce the ICT fluorescence efficiency of **1**, the concomitant electronic perturbation by triggering the PET process should be the main origin for the observed fluorescence quenching for **1DPA**. The occurrence of intramolecular PET is in principle facilitated by the deconjugation process between the electron donor and acceptor.[3] When compared with the monoaza-crown-derived stilbene probes,[5,35] the dpa amino nitrogen atom in **1** does not directly participate in the binding of metal ions, but the latter cases show much larger spectral responses. The participation of the PET process in the latter but not the former cases is apparently responsible. Since a reduction of fluorescence quantum yield is often observed for dpa-substituted arenes upon interacting with Zn(II) or other metal ions,[12,13] a similar PET process might be operative in some of these cases. Both the structural and electronic aspects elucidated herein should shed light on the future design of new fluoroionophores and light-emitting materials based on dpa-incorporated aromatic systems.

Experimental Section

Methods. The X-ray crystal structures were determined at room temperature. Intensity data were collected in 1315 frames with increasing ω (0.3° per frame) and corrected for *Lp* and absorption effects, using the SADABS program. The structures were solved by direct methods. Structural parameters were refined based on F^2. All calculations were performed by using SHELXTL programs. All non-hydrogen atoms were refined anisotropically. Hydrogen atoms were assigned idealized locations and given isotropic thermal parameters 1.2× the thermal parameter of the carbon atoms (but 1.5× for the hydrogens in methyl groups) to which they were attached. UV−vis absorption spectra and corrected fluorescence spectra were recorded at room temperature. A N_2-bubbled solution of anthracene (Φ_f = 0.27 in hexane)[36] was used as a standard for the fluorescence quantum yield determinations of **1**−**3** in acetonitrile under N_2-bubbled conditions with solvent refractive index correction. The optical density of all solutions was about 0.1 at the wavelength of excitation, and an error of ±10% is estimated for the fluorescence quantum yields. Fluorescence sensing measurements were performed in 1×10^{-5} M acetonitrile solutions in all cases. The fluorescence four-wall cuvette was charged with 3 mL of **1**−**3** and a magnetic stir bar. Aliquots of freshly prepared Zn(II) solution (0.01 M of $Zn(ClO_4)_2 \cdot 6H_2O$ in acetonitrile) were added at the prescribed increments. Solutions were allowed to equilibrate for 15 min before taking the measurement. Experimentation with longer equilibration times did not produce noticeable differences.

Materials. Solvents for organic synthesis were reagent grade or HPLC grade but all were HPLC grade for spectra and quantum yield measurements. All other compounds were purchased from a commercial source and were used as received. Compounds **1DMA**,[5] **1H**,[9] **2H**,[37] **4Br**,[38] **4CN**,[39] **5CN**,[39] **5Br**,[38] **6**,[40] and **7**[5] have been previously reported, and our melting points and/or ^{1}H NMR spectra conform to the literature values. The characterization data for the other compounds are provided in the Supporting Information. Typical synthetic procedures are as follows:

General Proceduces of Wittig Reaction for Substituted Stilbenes. A mixture of 5−25 mmol of phospohonium halide salt and 4-substituted benzaldehyde (0.9−1.0 equiv) and 0.5 g of tetrabutylammonium iodide in 20−50 mL of methylene chloride in a round-bottom flask was slowly added to 10−15 mL of a 50% (w/w) aqueous solution of potassium carbonate. In some cases the solution turned pink during the addition of base. The solution was then stirred at ambient temperature overnight. The organic layer became transparent at the top and the alkaline aqueous layer became turbid at the bottom

(35) Dumon, P.; Jonusauskas, G.; Dupuy, F.; Pée, P.; Rullière, C.; Létard, J.-F.; Lapouyade, R. *J. Phys. Chem.* **1994**, *98*, 10391−10396.
(36) Dawson, W. R.; Windsor, M. W. *J. Phys. Chem.* **1968**, *72*, 3251−3260.
(37) Mann, F. G.; Watson, J. *J. Org. Chem.* **1948**, *13*, 502−529.
(38) Everard, K. B.; Kumar, L.; Sutton, L. E. *J. Chem. Soc.* **1951**, 2807−2815.
(39) Hanna, P. E.; Gammans, R. E.; Sehon, R. D.; Lee, M.-K. *J. Med. Chem.* **1980**, *23*, 1038−1044.
(40) Fuson, R. C.; Cooke, H. G., Jr. *J. Am. Chem. Soc.* **1940**, *62*, 1180−1183.

of the flask. The two layers were separated and the aqueous layer was extracted with methylene chloride three times. The combined organic layer was washed with distilled water or brine and then dried over anhydrous $MgSO_4$. The solid residue after evaporation of the solvent was chromatographied with 1:2 ethyl acetate:hexane as eluent to remove the side product triphenylphosphine oxide. The resulting mixture of trans and cis isomers was recrystallized in $CHCl_3$/MeOH to afford the trans isomer. The filtrate that contains mainly the cis isomer was added with a catalytic amount of I_2 for cis → trans isomerization. The precipitate of trans isomer was filtered and then recrystallized in $CHCl_3$/MeOH. The yield was determined based on the total amount of trans isomer obtained.

General Procedures for Nitro → Amino Transformations. A heterogeneous mixture of 1−5 mmol of nitrostilbene and 5 equiv of $SnCl_2 \cdot 2H_2O$ in 15−40 mL of anhydrous ethanol was heated at 70 °C under nitrogen for 18 h. The solution was allowed to cool and then poured into 15−30 g of ice. The solution was made slightly basic by addition of 5% $NaHCO_{3\,(aq)}$ followed by extraction with ethyl acetate. The organic layer was washed with brine twice and then dried over magnesium sulfate. Evaporation of the solvent provided the crude product of aminostilbene. Further purification was performed by column chromatography.

General Procedures for Pd-Catalyzed Amination Reactions. As illustrated by the formation of compound **1Br**, compound **5Br** (0.20 g, 0.73 mmol), 2-bromopyridine (157 μL, 1.6 mmol), $NaOBu^t$ (0.20 g, 2.04 mmol), DPPF (0.032 g, 0.058 mmol), and $Pd_2(dba)_3$ (0.022 g, 0.024 mmol) in 3 mL of anhydrous toluene under argon weres heated at 100 °C for 24 h. The solution was cooled and then 25∼30 mL of CH_2Cl_2 was added. The insoluble residue was filtered off and the filtrate was concentrated under reduced pressure to afford the crude product. Further purification was performed by column chromatography, using a mixed solvent ethyl acetate/hexane (1:2) as the eluent to provide the light yellow solid with a yield of 57%.

Synthesis of 1-(*N,N*-Bis(2-pyridyl)amino)-4-nitrobenzene (2NO). A mixture of 4-nitroaniline (1.38 g, 10 mmol), 2-bromopyridine (2.93 mL, 30 mmol), KOH (1.80 g, 32 mmol), and $CuSO_4$ (0.052 g, 0.032 mmol) in a 50-mL flask was heated under argon at 180 °C for 16 h. After the reaction mixture was cooled to ambient temperature, dichloromethane and water were added to dissolve the solids. The organic layer was dried over anhydrous $MgSO_4$. The filtrate was concentrated under reduced pressure. Column chromatography with ethyl acetate/hexane (1:1) as eluent afforded **2NO** (11% yield).

Synthesis of *trans*-4-(*N,N*-Diphenylamino)-4′-(hydroxymethyl)stilbene (3OH). To a solution of **7** (1.28 g, 3.16 mmol) in 30 mL of THF at 0 °C was added slowly LAH (0.24 g, 6.32 mmol). The mixture was stirred for 2 h and then cold water was added dropwise to quench any unreacted LAH. The THF was removed under reduced pressure and the residue was then dissolved in ethyl acetate and washed with brine. The organic layer was dried over anhydrous $MgSO_4$ and the filtrate was concentrated under reduced pressure. Purification was performed by column chromatography (ethyl acetate:hexane = 1:5) and followed by recrystallization in CH_2Cl_2/hexane (0.63 g, 91% yield).

Synthesis of *trans*-4-(*N,N*-Diphenylamino)-4′-(*N*-phthalimidomethyl)stilbene (3PI). A mixture of **3OH** (0.28 g, 0.75 mmol), triphenylphosphine (0.30 g, 1.13 mmol), and phthalimide (0.17 g, 1.13 mmol) in 4.7 mL of THF was added dropwise to the THF solution (0.52 mL) of diisopropyl azadicarboxylate (DIAD) (0.23 g, 1.14 mmol). The mixture was stirred at room temperature for 16 h and the solvent was removed under reduced pressure. Column chromatography with ethyl acetate/hexane (1:6) afforded the desired product (0.63 g, 78% yield).

Synthesis of *trans*-4-(Aminomethyl)-4′-(*N,N*-diphenylamino)stilbene (3NH). A mixture of **3PI** (0.30 g, 0.59 mmol) and hydrazine (2.0 mL, 5.92 mmol) in 98 mL of ethanol was refluxed for 30 min. The resulting precipitate was filtered off and the filtrated was concentrated under reduced pressure. The crude product was recrystallized in CH_2Cl_2/hexane to afford the desired product (0.28 g, yield 88%).

Typical Procedures for the Preparation of $ZnCl_2$ Complexes. A mixture of dpa-substituted arenes (0.05 g) and $ZnCl_2$ (1.5 equiv) in 10 mL of acetonitrile or methanol was heated under argon at 90 °C for 2 h. The solution was cooled and then the solvent was removed under reduced pressure. The residue was washed with dichloromethane and distilled water and then recrystallized from methanol/acetonitrile to afford colorless crystals with a yield of 50%.

Acknowledgment. We thank the UST and the National Science Council of Taiwan, ROC, for financial support (NSC 91-2113-M-008-011 and NSC 92-2113-M-008-006), Professor S.-L. Wang (NTHU) for assistance in X-ray crystallography, and the reviewers for helpful comments.

Supporting Information Available: Crystal structures and structure refinement data, Cartesian coordinates of AM1-optimized structures, and detailed characterization data and ^1H and ^{13}C NMR spectra of new compounds; X-ray experimental details (CIF). This material is available free of charge via the Internet at http://pubs.acs.org.

JO049902Z